JOURNAL OF GUIDANCE, CONTROL, AND DYNAMICS
Vol. 30, No. 2, March–April 2007

Optimal Multi-Objective Linearized Impulsive Rendezvous

Ya-Zhong Luo,* Guo-Jin Tang,† and Yong-Jun Lei‡
National University of Defense Technology, 410073 Changsha, People's Republic of China

DOI: 10.2514/1.21433

The multi-objective optimization of linearized impulsive rendezvous is investigated in this paper and this optimization includes the minimum characteristic velocity, the minimum time of flight, and the maximum safety performance index, of which the trajectory safety performance index is defined as the minimum relative distance between a chaser and a target in the chaser's free-flying path. A theoretical model for calculating this safety performance index is provided. The three-objective optimization model is proposed based on the Clohessy–Wiltshire system, wherein a generalized inverse matrix solution for linear equations is applied to avoid handling the terminal equality constraints. The multi-objective nondominated sorting genetic algorithm is employed to obtain the Pareto solution set. The proposed approach is evaluated using the −V-bar homing and +V-bar homing rendezvous missions. It is shown that tradeoffs between time of flight, fuel cost, and passive trajectory safety for rendezvous trajectory is quickly demonstrated by the approach. By identifying multiple solutions, the approach can produce a variety of missions to meet different needs.

I. Introduction

THE optimal multiple-impulse spacecraft rendezvous problem has been studied extensively by a number of groups, such as Prussing [1,2], Gross and Prussing [3], Jones , and Prussing and Chiu [5], and recently by Shen and Tsiotras [6], Kim and Spencer [7], Prussing [8], Carter and Brient [9], Carter and Alvarez [10], Kechichian [11], Xiang and Xiao [12], and Coverstone-Carrol and Prussing [13]. Most of these works focused specifically on fuel-optimal time-fixed impulsive rendezvous problem. Recently, Luo et al. [14] reported the time-optimal impulsive rendezvous with impulse constraints.

Several criteria need to be considered when designing rendezvous trajectories, of which the total velocity characteristic is the typical measure of performance. However, the total velocity characteristic is not the single desired criterion and minimizing time of flight serves as an equally attractive mission objective. In addition, trajectory safety is another important objective for designing a practical rendezvous mission, especially for an approach mission [15–18]. In this context, combining these three objectives forms a multi-objective optimization problem.

The main goal of this study is to examine the trade relationship between the total characteristic velocity, the time of flight, and the trajectory safety performance index by multi-objective genetic algorithm (MOGA). A three-objective rendezvous optimization model is established based on the linearized rendezvous system. To obtain the Pareto solution set, we introduce one representative MOGA to solve the multi-objective optimization design problem.

II. Multi-Impulse Rendezvous Problem Using C–W Equations

The relative dynamics motion for rendezvous is typically illustrated by the well-known Clohessy–Wiltshire (C–W) equations, which is set up in a rotating orbit coordinate frame that is fixed to the target spacecraft as shown in Fig. 1.

$$\left.\begin{array}{c}\ddot{x}-2\omega\dot{y}=u_x\\ \ddot{y}+2\omega\dot{x}-3\omega^2 y=u_y\\ \ddot{z}+\omega^2 z=u_z\end{array}\right\} \tag{1}$$

where ω is the orbital rate of the target spacecraft, x, y, and z are the position components of the chase spacecraft, and u_x, u_y, and u_z are the thrust-acceleration components of the chase spacecraft.

Denoting the state vector $\boldsymbol{X}=(x\ \ y\ \ z\ \ \dot{x}\ \ \dot{y}\ \ \dot{z})^T$, the control vector $\boldsymbol{U}=(u_x,u_y,u_z)^T$, Eqs. (1) are revised as follows:

$$\dot{\boldsymbol{X}}=\mathbf{A}\boldsymbol{X}+\mathbf{B}\boldsymbol{U} \tag{2}$$

where

$$\mathbf{A}=\begin{pmatrix}0&0&0&1&0&0\\0&0&0&0&1&0\\0&0&0&0&0&1\\0&0&0&0&2\omega&0\\0&3\omega^2&0&-2\omega&0&0\\0&0&-\omega^2&0&0&0\end{pmatrix},\qquad \mathbf{B}=\begin{pmatrix}0&0&0\\0&0&0\\0&0&0\\1&0&0\\0&1&0\\0&0&1\end{pmatrix}$$

From Eqs. (2), the state transition matrix is obtained

$$\boldsymbol{\Phi}(t,t_0)=\begin{pmatrix}1&6(\rho-\sin\rho)&0&\frac{4\sin\rho-3\rho}{\omega}&\frac{2(1-\cos\rho)}{\omega}&0\\0&4-3\cos\rho&0&\frac{-2(1-\cos\rho)}{\omega}&\frac{\sin\rho}{\omega}&0\\0&0&\cos\rho&0&0&\frac{\sin\rho}{\omega}\\0&6\omega(1-\cos\rho)&0&4\cos\rho-3&2\sin\rho&0\\0&3\omega\sin\rho&0&-2\sin\rho&\cos\rho&0\\0&0&-\omega\sin\rho&0&0&\cos\rho\end{pmatrix} \tag{3}$$

where $\rho=\omega(t-t_0)$.

Let

$$\boldsymbol{\Phi}(t,t_0)=\begin{pmatrix}\boldsymbol{\Phi}_{11}&\boldsymbol{\Phi}_{12}\\\boldsymbol{\Phi}_{21}&\boldsymbol{\Phi}_{22}\end{pmatrix} \tag{4}$$

Also, define position- and velocity-related partitions as

$$\boldsymbol{\Phi}_p(t,t_0)=\begin{pmatrix}\boldsymbol{\Phi}_{11}\\\boldsymbol{\Phi}_{21}\end{pmatrix}\qquad \boldsymbol{\Phi}_v(t,t_0)=\begin{pmatrix}\boldsymbol{\Phi}_{12}\\\boldsymbol{\Phi}_{22}\end{pmatrix} \tag{5}$$

Received 28 November 2005; revision received 18 May 2006; accepted for publication 2 June 2006.

*Corresponding Author, Ph.D. Candidate, College of Aerospace and Material Engineering, Department of Aerospace Science and Technology, Student Member AIAA; E-mail: yzluo@sohu.com.

†Professor, College of Aerospace and Material Engineering, Department of Aerospace Science and Technology.

‡Associate Professor, College of Aerospace and Material Engineering, Department of Aerospace Science and Technology.

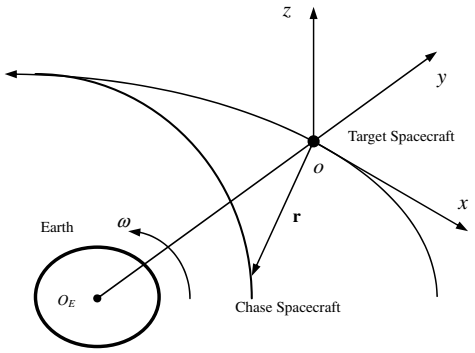

Fig. 1 Orbit coordinate system.

Equations (2) denote a linear homogeneous system, and its special solution satisfying $\boldsymbol{X}(t_0) = \boldsymbol{X}_0$ is:

$$\boldsymbol{X}(t) = \boldsymbol{\Phi}(t, t_0)\boldsymbol{X}_0 + \int_{t_0}^{t} \boldsymbol{\Phi}_v(t, s)\boldsymbol{U}(s)\,\mathrm{d}s \tag{6}$$

For a rendezvous mission, the initial state conditions are defined

$$\boldsymbol{X}(t_0) = \boldsymbol{X}_0 \tag{7}$$

Also, the final state conditions are defined

$$\boldsymbol{X}(t_f) = \boldsymbol{X}_f \tag{8}$$

where t_0 and t_f are the initial and terminal time for a rendezvous mission.

The thrust can be approximated as N impulses:

$$\boldsymbol{U}(t) = \sum_{i=1}^{N} \Delta\mathbf{v}_i \delta(t - t_i) \tag{9}$$

where t_i is the time when an impulse is applied, $\Delta\mathbf{v}_i = (\Delta v_{xi}, \Delta v_{yi}, \Delta v_{zi})^T$ $(i = 1, 2, \cdots, N)$. Substituting Eqs. (9) into Eqs. (6), we get

$$\boldsymbol{X}(t_f) = \boldsymbol{\Phi}(t_f, t_0)\boldsymbol{X}_0 + \sum_{i=1}^{N} \boldsymbol{\Phi}_v(t_f, t_i)\Delta\mathbf{v}_i \tag{10}$$

Let

$$\Delta\boldsymbol{X} = \boldsymbol{X}(t_f) - \boldsymbol{\Phi}(t_f, t_0)\boldsymbol{X}(t_0) \qquad (6 \times 1) \tag{11}$$

$$\Delta\mathbf{V} = [(\Delta\mathbf{v}_1)^T(\Delta\mathbf{v}_2)^T \cdots (\Delta\mathbf{v}_N)^T]^T \qquad (3N \times 1) \tag{12}$$

$$\mathbf{F} = [\boldsymbol{\Phi}_v(t_f, t_1)\boldsymbol{\Phi}_v(t_f, t_2) \cdots \boldsymbol{\Phi}_v(t_f, t_N)] \qquad (6 \times 3N) \tag{13}$$

Then

$$\Delta\boldsymbol{X} = \mathbf{F}\Delta\mathbf{V} \tag{14}$$

When $N = 1$, Eq. (14) has no solution, generally.

Let $[\mathbf{F}, \Delta\boldsymbol{X}]$ be the augmented matrix of the system of linear equations described as Eq. (14). If $\mathrm{rank}([\mathbf{F}, \Delta\boldsymbol{X}]) = \mathrm{rank}(\mathbf{F})$, Eq. (14) has a solution; otherwise, not. Hereafter, we assume it has a solution.

When $N = 2$ (two-impulse rendezvous), by Eq. (14)

$$\Delta\mathbf{V} = \mathbf{F}^{-1}\Delta\boldsymbol{X} \tag{15}$$

When $N > 2$, Eq. (11) has more than one solution. Its general solution is

$$\Delta\mathbf{V} = \mathbf{F}^{-}\Delta\boldsymbol{X} + (\mathbf{I} - \mathbf{F}^{-}\mathbf{F})\boldsymbol{\xi} \tag{16}$$

where $\mathbf{F}^{-}$ is an arbitrary generalized inverse matrix of $\mathbf{F}$, $\boldsymbol{\xi}$ is an arbitrary $3N \times 1$ vector.

If the minimum-norm solution is chosen, the N-impulse vector is obtained

$$\Delta\mathbf{V} = \mathbf{F}^T(\mathbf{F}\mathbf{F}^T)^{-1}\Delta\boldsymbol{X} \tag{17}$$

The minimum-norm solution is different from the minimum-fuel solution [12]. By optimizing $\boldsymbol{\xi}$, the minimum-fuel solution can be obtained with the minimum-norm solution as the initial guess.

III. Trajectory Safety Performance

A rendezvous mission can be divided into a number of major phases: launch, phasing, far-range rendezvous (homing rendezvous), close-range rendezvous, and mating [15]. The discussions concerning trajectory safety concentrate on the rendezvous phase because the mission phases of launch and phasing are generally controlled by operators or computer functions on the ground. Generally, two categories are considered in the rendezvous trajectory safety: active trajectory protection and passive trajectory protection. Active trajectory protection focuses on designing an approximate active collision avoidance maneuver, and more details on this issue can be found in [15]. On the other hand, passive trajectory protection centers on designing all trajectory elements in an approach trajectory sequence such that if, at any point of the trajectory, thrust control ceases, the resulting "free trajectory" will remain collision-free for a time to be defined (TBD). In our optimal multi-objective rendezvous design, only passive trajectory protection is considered.

Assume the chaser has lost control at any time $\tau_0 (t_0 \le \tau_0 \le t_f)$ during the rendezvous trajectory. Based on the C–W equations, its free-flying position at time τ is found to be the analytical function of the initial position $\boldsymbol{X}_{\tau 0} = (x_{\tau 0}, y_{\tau 0}, z_{\tau 0})^T$ and the initial velocity $\dot{\boldsymbol{X}} = (\dot{x}_{\tau 0}, \dot{y}_{\tau 0}, \dot{z}_{\tau 0})^T$ at time τ_0

$$\begin{cases} x(\tau) = \left(x_{\tau 0} + \frac{2\dot{y}_{\tau 0}}{\omega}\right) + 2\left(\frac{2\dot{x}_{\tau 0}}{\omega} - 3y_{\tau 0}\right)\sin(\omega\Delta\tau) - 2\frac{\dot{y}_{\tau 0}}{\omega}\cos(\omega\Delta\tau) - (3\dot{x}_{\tau 0} - 6\omega y_{\tau 0})\Delta\tau \\ y(\tau) = \left(4y_{\tau 0} - 2\frac{\dot{x}_{\tau 0}}{\omega}\right) + \frac{\dot{y}_{\tau 0}}{\omega}\sin(\omega\Delta\tau) - \left(3y_{\tau 0} - 2\frac{\dot{x}_{\tau 0}}{\omega}\right)\cos(\omega\Delta\tau) \\ z(\tau) = \frac{\dot{z}_{\tau 0}}{\omega}\sin(\omega\Delta\tau) + z_0\cos(\omega\Delta\tau) \end{cases} \tag{18}$$

where $\Delta\tau = \tau - \tau_0$. The corresponding velocity is found to be

$$\begin{cases} \dot{x}(\tau) = 2(2\dot{x}_{\tau 0} - 3y_{\tau 0}\omega)\cos(\omega\Delta\tau) + 2\dot{y}_{\tau 0}\sin(\omega\Delta\tau) - 3\dot{x}_{\tau 0} + 6\omega y_{\tau 0} \\ \dot{y}(\tau) = \dot{y}_{\tau 0}\cos(\omega\Delta\tau) + (3\omega y_{\tau 0} - 2\dot{x}_{\tau 0})\sin(\omega\Delta\tau) \\ \dot{z}(\tau) = \dot{z}_{\tau 0}\cos(\omega\Delta\tau) - z_{\tau 0}\omega\sin(\omega\Delta\tau) \end{cases} \tag{19}$$

The corresponding acceleration is found to be

$$\begin{cases} \ddot{x}(\tau) = 2\omega(3y_{\tau 0}\omega - 2\dot{x}_{\tau 0})\sin(\omega\Delta\tau) + 2\omega\dot{y}_{\tau 0}\cos(\omega\Delta\tau) \\ \ddot{y}(\tau) = -\omega\dot{y}_{\tau 0}\sin(\omega\Delta\tau) + \omega(3\omega y_{\tau 0} - 2\dot{x}_{\tau 0})\cos(\omega\Delta\tau) \\ \ddot{z}(\tau) = -\omega\dot{z}_{\tau 0}\sin(\omega\Delta\tau) - z_{\tau 0}\omega^2\cos(\omega\Delta\tau) \end{cases} \tag{20}$$

The relative distance of the chaser to the target at time τ is defined as

$$r(\tau) = f(\boldsymbol{X}_{\tau 0}, \dot{\boldsymbol{X}}_{\tau 0}, \tau_0, \tau) = \sqrt{x(\tau)^2 + y(\tau)^2 + z(\tau)^2} \tag{21}$$

The minimum value of $r(\tau)$ is used to measure the safety of the drift trajectory. Let

$$r_{\min}(\tau_0) = \min_{\tau_0 \le \tau \le \tau_0 + \mathrm{TBD}} r(\tau) \tag{22}$$

In the study, TBD is $2\pi/\omega$, the same as the period of the target orbit.

The rendezvous trajectory has a time history from t_0 to t_f, thus τ_0 can be any point in the range of $t_0 \le \tau_0 \le t_f$. Let

$$r_{\text{safe}} = \min_{t_0 \le \tau_0 \le t_f} r_{\min}(\tau_0) \tag{23}$$

r_{safe} is regarded as the trajectory safety performance index. For a general passive-safe required rendezvous trajectory, r_{safe} should be larger than a defined value. From the point of view of optimal design, r_{safe} should be as large as possible. Therefore, r_{safe} is proposed as one design optimization objective function in the multi-objective rendezvous design,

$$\max J = r_{\text{safe}} \tag{24}$$

Through Eq. (23), the calculation of r_{safe} involves two functional optimization problems. Firstly, a semitheoretical model for calculating $r_{\min}(\tau_0)$ is provided.

Assume that $r(\tau)$ reaches its minimum at time τ^*, τ^* should satisfy the following two conditions:

$$\frac{dr}{d\tau^*} = 0, \qquad \frac{d^2r}{d\tau^{*2}} > 0 \tag{25}$$

From Eqs. (18–20)

$$\frac{dr}{d\tau} = \frac{(x\dot{x} + y\dot{y} + z\dot{z})}{r} \tag{26}$$

$$\frac{d^2r}{d\tau^2} = -\frac{(x\dot{x} + y\dot{y} + z\dot{z})^2}{r^3} + \frac{\dot{x}^2 + x\ddot{x} + \dot{y}^2 + y\ddot{y} + \dot{z}^2 + z\ddot{z}}{r} \tag{27}$$

If $dr/d\tau = 0$, Eq. (27) is revised to

$$\frac{d^2r}{d\tau^2} = \frac{\dot{x}^2 + x\ddot{x} + \dot{y}^2 + y\ddot{y} + \dot{z}^2 + z\ddot{z}}{r} \tag{28}$$

Based on the above analyses, the iteration method to calculate $r_{\min}(\tau_0)$ is described as follows:

Step 1: give an initial guess τ^0, and iteration = 0.

Step 2: solve $dr/d\tau = 0$ by Newton–Raphson method and obtain one solution τ^*.

Step 3: if $d^2r/d\tau^{*2} > 0$, τ^* is the true solution, stop; otherwise, go to Step 4.

Step 4: let $\tau^0 = (\tau^* + \tau^0)/2$, iteration+ = 1. If iteration < iteration max, go to Step 2; otherwise, go to Step 5.

Step 5: make $\tau^* = \tau^0$ the true solution.

After $r_{\min}(\tau_0)$ is defined, one simplified method is used to calculate r_{safe}. A number of points $(\tau_{0,1}, \tau_{0,2}, \ldots, \tau_{0,l})$ are chosen in the range of $[t_0, t_f]$ at equal time interval. Each $r_{\min}(\tau_{0,i})$ corresponds to $\tau_{0,i}$ is calculated, then

$$r_{\text{safe}} = \min[r_{\min}(\tau_{0,1}), \ldots, r_{\min}(\tau_{0,l})] \tag{29}$$

IV. Multi-Objective Optimization Model

Based on the linearized rendezvous equations (1–17), a multi-objective optimization model for an N-impulse rendezvous is provided.

A. Objective Function Vector

The time of flight is chosen as the first objective function:

$$\min f_1(\boldsymbol{x}) = t_f \tag{30}$$

The total velocity characteristic is the second objective function:

$$\min f_2(\boldsymbol{x}) = \Delta v = \sum_{i=1}^{N} |\Delta \mathbf{v}_i| \tag{31}$$

The third objective function is the trajectory safety performance index

$$\min f_3(\boldsymbol{x}) = -r_{\text{safe}} \tag{32}$$

B. Optimization Variables

Because it is the minimum-time rendezvous, t_f is an optimization variable. The impulse times $t_i (i = 1, 2, \ldots, N)$ are also optimization variables. To improve optimization performance, the variable-scaling method is imposed on t_i. Let

$$\alpha_i = t_i/t_f \qquad 0 \le \alpha_i \le 1 \tag{33}$$

If $\Delta\mathbf{V}$ is chosen as the optimization variables, it is required to handle equality constraints as described by Eqs. (8). As is well known, the equality constraint is very difficult to handle for almost all optimization algorithms. To overcome this problem, the generalized inverse matrix solution for a linear equation group is applied, i.e., the impulse vector is defined directly by Eqs. (16) or Eqs. (17) when $t_i (i = 1, 2, \ldots, N)$ are determined. By using this method, the terminal equality constraints are satisfied naturally. Herein, the minimum-norm inverse matrix is adopted as the generalized inverse matrix, i.e., $\mathbf{F}^- = \mathbf{F}^T(\mathbf{F}\mathbf{F}^T)^{-1}$.

In total, the optimization vector $\boldsymbol{x}$ includes three parts: one part is t_f, the second part is $(\alpha_1, \ldots, \alpha_N)^T$, and the third part is $\boldsymbol{\xi}$.

If $N = 2$, then $\mathbf{F}^- = \mathbf{F}^{-1}$, $\boldsymbol{x} = (t_f, \alpha_1, \alpha_2)^T$. If $N > 2$

$$\boldsymbol{x} = \begin{cases} (t_f, \alpha_1, \ldots, \alpha_N, \boldsymbol{\xi})^T & \Delta\mathbf{V} \text{ is defined by the general solution Eqs. (16)} \\ (t_f, \alpha_1, \ldots, \alpha_N)^T & \Delta\mathbf{V} \text{ is defined by the minimum-norm solution Eqs. (17)} \end{cases} \tag{34}$$

C. Constraints

One kind of impulse constraints is considered: the time of impulse. The general constraint on $t_i (i = 1, 2, \ldots, N)$ is

$$t_0 \le t_1 < t_2 \cdots < t_N \le t_f \tag{35}$$

For the practical rendezvous mission, it is necessary to adjust the attitude before firing the engine, and this requirement constrains the interval time between two arbitrary impulses. The constraint is formulated as follows:

$$t_{i+1} - t_i \ge \Delta t \qquad (i = 1, 2, \ldots, N-1) \tag{36}$$

V. Multi-Objective Genetic Algorithms

A. Problem Formulation

A general multi-objective optimization problem is to find the design variables that optimize a vector objective function over the feasible design space. The objective functions are the quantities that the designer wishes to minimize, maximize, or attain a certain value. The problem formulation in standard form for a minimization is given here, which is similar for the other cases [19].Minimize

$$\mathbf{f}(\boldsymbol{x}) = [f_1(\boldsymbol{x}), f_1(\boldsymbol{x}), \ldots, f_m(\boldsymbol{x})]^T \tag{37a}$$

subject to

$$\mathbf{g}(\boldsymbol{x}) = [g_1(\boldsymbol{x}), g_2(\boldsymbol{x}), \ldots, g_p(\boldsymbol{x})]^T \le 0 \tag{37b}$$

where

$$\boldsymbol{x} = (x_1, x_2, \ldots, x_n)^T \in \boldsymbol{x} \subset \mathbf{R}^n \tag{37c}$$

B. Concept of Pareto Optimal [19]

As shown in Eqs. (37), the design objectives of a multi-objective optimization problem are at least partly conflicting. For this reason, a multi-objective optimization problem normally does not have a single optimal solution. Instead, the solution is the family of designs named the Pareto-optimal set. The definition of the Pareto-optimal solution is stated as follows.

In a minimization problem, a feasible design $\boldsymbol{x}^a$ is said to be inferior with respect to another feasible design point $\boldsymbol{x}^b$ if

$$f_i(\boldsymbol{x}^b) \le f_i(\boldsymbol{x}^a), \qquad i = 1, \ldots, m \tag{38}$$

with a strict inequality for at least one i. Correspondingly, the design point $\boldsymbol{x}^b$ is said to dominate $\boldsymbol{x}^a$. If $\boldsymbol{x}^b$ neither dominates nor is inferior to $\boldsymbol{x}^a$, then $\boldsymbol{x}^a$ and $\boldsymbol{x}^b$ are said to be noninferior with respect to each other.

For a population of design points, a feasible design solution $\boldsymbol{x}^*$ is called a Pareto-optimal solution if it is not inferior with respect to any other feasible design points.

C. MOGA

Genetic algorithms are a global search method that mimics the behavior observed in biological populations. Genetic algorithms employ the principle of survival of the fittest in their search processes and have been applied successfully to the design of many complex systems. To perform the optimization process, genetic algorithms employ three operators to propagate the population of possible parameter values from one generation to another: selection operator, crossover operator, and mutation operator.

MOGA is a genetic algorithm (GA) extended for multi-objective optimization. GAs solve a single-objective optimization problem by emulating the natural evolutionary process in which a population of design points (or individuals) is iteratively evolved to reach an optimum solution. In GAs, at each iteration, the probability that an individual is selected to evolve is governed by its fitness value, which is a function of that individual's single-objective value and its constraint values. MOGA extends a genetic algorithm's fitness assignment method so that it is applicable to multiple objectives [20]. There are many variants of MOGA reported in the literature, for example, Schaffer [21], Fonseca and Fleming [22], Srinivas and Deb [23], Narayanan and Azarm [24], and Crossley et al. [25]. Other MOGAs can be found in Deb's book [20]. Among these MOGAs, the nondominated sorting genetic algorithm (NSGA) developed by Srinivas and Deb [23] is widely used. Coverstone–Carroll et al. [26] have successfully applied the NSGA to generate fronts of Pareto-optimal trajectories for both Earth–Mars and Earth–Mercury missions. NSGA-2 [27] was advanced from its origin, NSGA. In NSGA-2, a fast-nondominated sorting approach is used for each individual to create Pareto rank, and a crowding distance assignment is applied to implement density estimations.

In next section, the model of the NSGA-2 used in our study is presented.

D. Brief Description of the NSGA-2

The algorithm is based on the idea of transforming the m objectives to a single fitness measure by the creation of a number of fronts, sorted according to nondomination. During fitness assignment, the first front is created as the set of solutions is not dominated by any solutions in the population. These solutions are given the highest fitness and temporarily removed from the population. After this, a second nondominated front consisting of the solutions that are now nondominated is built, assigned the second-highest fitness, etc. This is repeated until each of the solutions have been assigned a fitness. After each front has been created, its members are assigned crowding distances (normalized distance to closest neighbors in the front in the objective space) later to be used for niching. Readers are referred to [20,27] for more details of the NSGA-2.

The real-coded method is adopted in our work. Unlike the original edition of NSGA-2, the arithmetical crossover operator and the nonuniform mutation operator [28] are applied. Selection is performed in tournaments of size two: the solution with the lowest front number wins. If the solutions come from the same front, the solution with the highest crowding distance wins, because a high distance to the closest neighbors indicates that the solution is located at a sparse part of the front. The constraint handling method of Deb et al. [27] is adopted. Feasible, noninferior designs are stored in an approximate Pareto set that is updated after each generation as new designs dominating previously stored designs are found.

VI. Examples

A. Problem Configuration

Many rendezvous missions have been determined in this work using the NSGA-2. In this paper, the homing rendezvous missions are selected to demonstrate our approach. The homing rendezvous can also be named far-range rendezvous [15]. The major objective of the homing rendezvous phase is the reduction of trajectory dispersions, i.e., the achievement of position, velocity, and angular rate conditions, which are necessary for the initiation of the close-range rendezvous operations. Passive trajectory safety is one important performance index for designing a homing rendezvous trajectory. In this section, two representative homing rendezvous trajectories are analyzed and compared: $-$V-bar homing and $+$V-bar homing. The former requires the chaser to enter a position-hold point behind the target, and the latter, a position-hold point in front of the target.

Both of them have the same initial conditions:

$$\boldsymbol{X}_0 = (35713.3\ \text{m}, -13455.1\ \text{m}, -28.8\ \text{m}, -22.9\ \text{m/s}, 0.66\ \text{m/s}, -0.09\ \text{m/s})^T$$

Table 1 NSGA-2 parameters used in experiments

Parameter	Value
Coded-type	floating coded
Population size	100
Maximum number of generations	200
Selection type	tournament
Scale of tournament	2
Crossover type	arithmetical
Probability of crossover	0.92
Mutation type	nonuniform
Probability of mutation	0.10

Table 2 Problem configurations

Parameter	Value
Number of impulses	2,3,4, respectively
Time of flight t_f, s	search space [1000, 5000]
$\alpha_i (i = 1, 2, \ldots, N)$	search space [0, 1]
l (number of points selected to calculate r_{safe})	10
Δt, s	100

Table 3 Statistical results on number of Pareto-optimal solutions for the −V-bar homing rendezvous

Problem	Number of Pareto-optimal solutions			Success rate
	Maximum	Minimum	Mean	
Four-impulse	764	385	524.7	100%
Three-impulse	552	343	462.3	100%
Two-impulse	1316	809	1008.2	100%

The final conditions are different and for the −V-bar homing rendezvous are

$$\boldsymbol{X}_f = (2000\ \text{m}, 0, 0, 0, 0, 0)^T$$

Whereas the final conditions for the +V-bar homing rendezvous are

$$\boldsymbol{X}_f = (-2000\ \text{m}, 0, 0, 0, 0, 0)^T$$

In all test cases, the target spacecraft orbit is a 400 km circular orbit, which corresponds to an orbital rate ω of 0.00113 rad/s.

The parameters of the NSGA-2 used in experiments are provided in Table 1. The optimization variables are t_f and $\alpha_i (i = 1, 2, \ldots, N)$, thus the impulse vector is the minimum-norm solution. Other configurations of the optimal multi-objective rendezvous problem are provided in Table 2.

B. Pareto-Solution Sets

The NSGA-2 is used to optimize the two-, three-, and four-impulse −V-bar and +V-bar homing rendezvous trajectories, respectively. Considering the stochastic characteristic of the NSGA-2, ten independent runs for each test case are completed. Table 3 provides the statistical results on the number of the converged Pareto-optimal solutions obtained in each execution for the −V-bar homing rendezvous. Figures 2–4 illustrate several selected Pareto sets, in which the converged Pareto-optimal solutions are indicated with an "o" [f1 indicates total characteristic velocity (m/s), f2 indicates time of flight (s), and f3 indicates negtive minimum relative distance (m)]. Figure 2 compares the three-impulse +V-bar and −V-bar cases. Figure 3 compares the four- and three-impulse +V-bar cases. Figure 4 compares the three- and two-impulse −V-bar cases. The Pareto solutions provided by Figs. 2–4 are the solutions obtained in one of these ten runs. Table 4 lists three Pareto-optimal solutions for the four-impulse −V-bar homing rendezvous. Figure 5 illustrates the trajectory (including the time histories of the position and the velocity) corresponding with the first solution listed in Table 4. For this rendezvous trajectory, r_{safe} is obtained when the chaser has lost control during the first impulse and the second impulse. Figure 6 illustrates the chaser's free-flying path (starts at 495.8 s) in the x–y plane, and also the time history of the relative distance is provided.

C. Discussion

According to our experiments and the data provided by Tables 3 and 4 and Figs. 2–6, it is clear that the NSGA-2 has successfully generated the Pareto-optimal solution fronts. The proposed optimization model and the NSGA-2 are effective to solve the optimal multi-objective linearized impulsive rendezvous. The time cost of one run on a Dell computer with a 2.9 GHz CPU is about 90 s. The approach is quick and effective to provide very valuable insights into the tradeoffs available in the design space of the rendezvous trajectory.

In our study, only a single set of initial conditions is considered and the number of impulses is specified a priori rather than being a result of the optimization like that in [5]. Besides, the impulse vector is a minimum-norm solution. Therefore, it is beyond our scope to make generalizations about rendezvous solutions. Nevertheless, our current study on the test cases has generated several inherent principles regarding the optimal multi-objective rendezvous trajectory, which may also be useful for other cases:

1) There is an obvious relation between the time of flight and the total characteristic velocity; the longer rendezvous time would result in less fuel cost and vice versa. However, a relation is not apparent between the time of fight (or the total characteristic velocity) and the trajectory safety performance index.

2) As Fig. 2 demonstrated, the −V-bar has better passive trajectory safety performance than the +V-bar for three-impulse homing rendezvous. This is true for the four- and two-impulse cases. The range of r_{safe} for the −V-bar homing rendezvous is [1100, 2000] m, but [0, 2000] m for the +V-bar homing rendezvous.

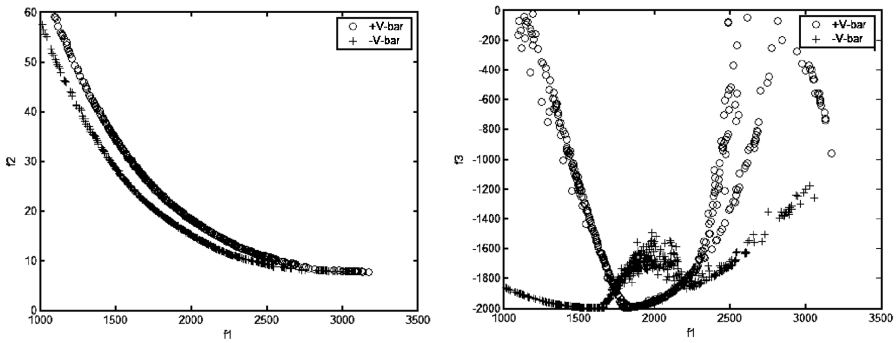

a) f1 vs f2 **b) f1 vs f3**

Fig. 2 Pareto sets for the three-impulse +V-bar and −V-bar homing rendezvous.

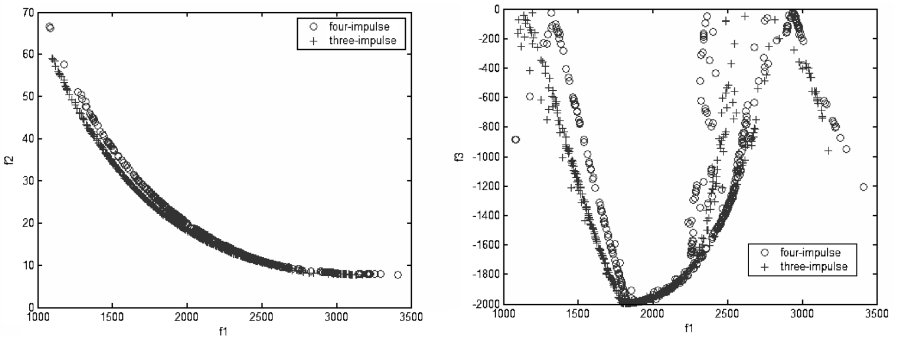

a) f1 vs f2 **b) f1 vs f3**

Fig. 3 Pareto sets for the four- and three-impulse +V-bar homing rendezvous.

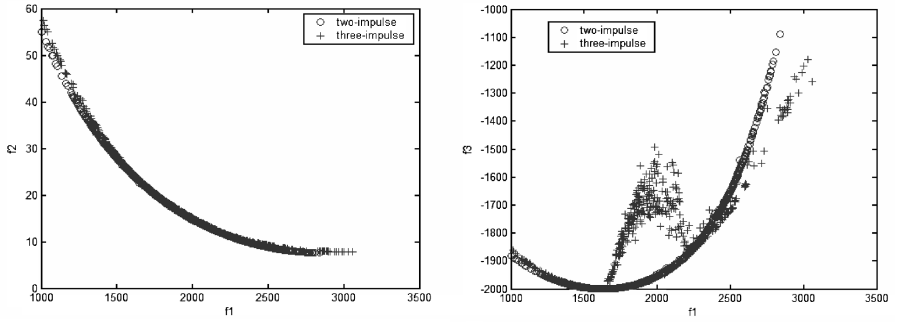

a) f1 vs f2 **b) f1 vs f3**

Fig. 4 Pareto sets for the two- and three-impulse −V-bar homing rendezvous.

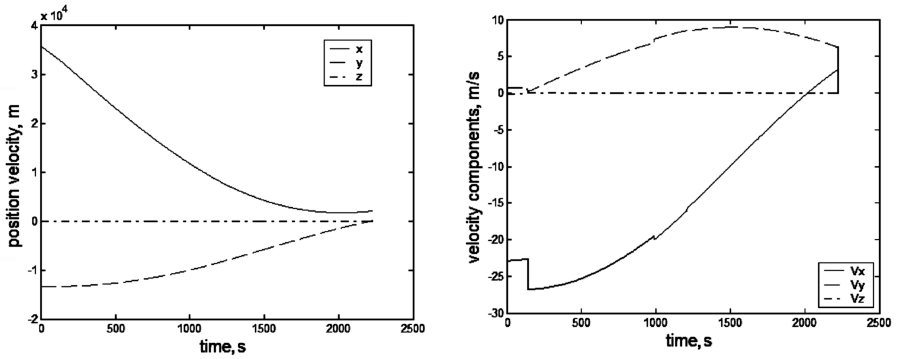

a) Time history of position components **b) Time history of velocity components**

Fig. 5 The rendezvous trajectory corresponding with the first solution listed in Table 4.

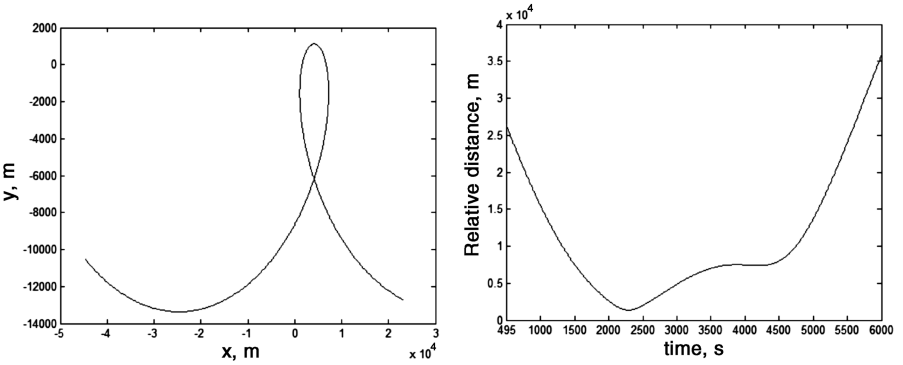

a) Flight path in x–y plane **b) Time history of relative distance (r_{safe} =1360.7 at 2285 s)**

Fig. 6 Chaser's free-flyer path corresponding with the first solution listed in Table 4.

Table 4 Three Pareto-optimal solutions for the four-impulse −V-bar homing rendezvous

Solution index	t_f, s	Δv, m/s	r_{safe}, m	$t_i (i = 1, 2, 3, 4)$, s
1	2231.0	12.2	1360.7	139.9, 988.8, 1209.5, 2225.2
2	2759.8	8.3	1523.2	175.0, 1214.2, 1493.8, 2752.1
3	2592.6	8.9	1657.8	162.8, 1204.8, 1406.2, 2587.1

3) For the same time of flight, the −V-bar rendezvous has less fuel cost compared with the +V-bar rendezvous. This can be explained that the latter has longer flight journey.

4) The fronts of the V-bar and −V-bar are similar for the two-impulse case, but different for the three-impulse and the four-impulse cases. The fronts of the three-impulse case and the four-impulse case are similar, but different from the two-impulse case. As the number of impulses increase, populations are distributed less evenly over apparent Pareto fronts.

5) As Figs. 3 and 4 demonstrated, the fuel cost is found to improve as the number of impulses increase with the same time of flight. However, this would not be always true for other cases. Some examples of multi-impulse rendezvous trajectory with less fuel cost than two-impulse rendezvous trajectory were provided by Prussing and Chiu [5].

VII. Conclusions

While other studies on optimal impulsive rendezvous are limited to one single-objective function (minimum fuel cost or minimum time), our optimal linearized impulsive rendezvous design incorporates three-objective functions including the minimum fuel cost, the minimum time of flight, and the maximum trajectory safety performance index. It is found that the nondominated sorting genetic algorithm-2 worked well for the optimal three-objective linearized impulsive rendezvous problem. Our studies provide a quick and effective tool to demonstrate the relation between time of flight, fuel cost, and passive trajectory safety for rendezvous trajectory. By identifying multiple solutions, the approach can produce a variety of missions to meet different needs.

References

[1] Prussing, J. E., "Optimal Four-Impulse Fixed-Time Rendezvous in the Vicinity of a Circular Orbit," *AIAA Journal*, Vol. 7, No. 5, 1969, pp. 928–935.

[2] Prussing, J. E., "Optimal Two- and Three-Impulse Fixed-Time Rendezvous in the Vicinity of a Circular Orbit," *AIAA Journal*, Vol. 8, No. 7, 1970, pp. 1221–1228.

[3] Gross, L. R., and Prussing, J. E., "Optimal Multiple-Impulse Direct Ascent Fixed-Time Rendezvous," *AIAA Journal*, Vol. 12, No. 7, 1974, pp. 885–889.

[4] Jones, J. B., "Optimal Rendezvous in the Neighborhood of a Circular Orbit," *Journal of the Astronautical Sciences*, Vol. 24, No. 1, 1976, pp. 55–90.

[5] Prussing, J. E., and Chiu, J. H., "Optimal Multiple-Impulse Time-Fixed Rendezvous Between Circular Orbits," *Journal of Guidance, Control, and Dynamics*, Vol. 9, No. 1, 1986, pp. 17–22.

[6] Shen, H. J., and Tsiotras, P., "Optimal Two-Impulse Rendezvous Using Multiple-Revolution Lambert Solutions," *Journal of Guidance, Control, and Dynamics*, Vol. 26, No. 1, 2003, pp. 50–61.

[7] Kim, Y. H., and Spencer, D. B., "Optimal Spacecraft Rendezvous Using Genetic Algorithms," *Journal of Spacecraft and Rockets*, Vol. 39, No. 6, 2002, pp. 859–865.

[8] Prussing, J. E., "A Class of Optimal Two-Impulse Rendezvous Using Multiple-Revolution Lambert Solutions," *Journal of the Astronautical Sciences*, Vol. 48, Nos. 2–3, 2000, pp. 131–148.

[9] Carter, T. E., and Brient, J., "Linearized Impulsive Rendezvous Problem," *Journal of Optimization Theory and Applications*, Vol. 86, No. 3, 1995, pp. 553–584.

[10] Carter, T. E., and Alvarez, S. A., "Quadratic-Based Computation of Four-Impulse Optimal Rendezvous Near Circular Orbit," *Journal of Guidance, Control, and Dynamics*, Vol. 23, No. 1, 2000, pp. 109–117.

[11] Kechichian, J. A., "The Algorithm of the Two-Impulse Time-Fixed Noncoplanar Rendezvous with Drag and Oblateness Effects," *Journal of the Astronautical Sciences*, Vol. 46, No. 1, 1998, pp. 47–64.

[12] Xiang, K. H., and Xiao, Y. L., "A Study of Propellant Consumption of Impulsive Maneuvers in Space Rendezvous," *Chinese Space Science and Technology*, Vol. 19. No. 3, 1999, pp. 9–15 (in Chinese).

[13] Taur, D. R., Coverstone–Carrol, V., and Prussing, J. E., "Optimal Impulse Time-Fixed Orbital Rendezvous and Interception with Path Constraints," *Journal of Guidance, Control, and Dynamics*, Vol. 18, No. 1, 1995, pp. 54–60.

[14] Luo, Y. Z., Tang, G. J., and Li, H. Y., "Optimization of Multiple-Impulse Minimum-Time Rendezvous with Impulse Constraints Using a Hybrid Genetic Algorithm," *Aerospace Science and Technology* [online journal], Vol. 10, No. 6, pp. 534–540, http://www.sciencedirect.com/science/journal/12709638 [cited Aug. 2006].

[15] Fehse, W., *Automated Rendezvous and Docking of Spacecraft*, Cambridge Univ. Press, New York, 2003, pp. 9–17, 77–112.

[16] Yamanaka, K., Yokota, K., Yamada, K., Yoshikawa, S., Koyama, H., Tsukahara, K., and Nakamura, T., "Guidance and Navigation System Design of R-bar Approach for Rendezvous and Docking," *17th International Communications Satellite Systems Conference and Exhibit*, 1998; also AIAA Paper 98-19040.

[17] Marsh, S. M., and White, B. D., "Trajectory Design and Navigation Analysis for Cargo Transfer Vehicle Proximity Operations," *AIAA/AAS Astrodynamics Conference*, 1992; also AIAA Paper 92-4436-CP.

[18] Roger, A. B., and McInnes, C. R., "Safety Constrained Free-Flyer Path Planning at the International Space Station," *Journal of Guidance, Control, and Dynamics*, Vol. 23, No. 6, 2000, pp. 971–979.

[19] Gunawan, S., Azarm, S., and Wu, J., "Quality-Assisted Multi-Objective Multidisciplinary Genetic Algorithms," *AIAA Journal*, Vol. 41, No. 9, 2003, pp. 1752–1762.

[20] Deb, K., *Multi-Objective Optimization Using Evolutionary Algorithms*, Wiley, Chichester, U.K., 2002, pp. 171–285.

[21] Schaffer, J. D., "Multiple Objective Optimization with Vector Evaluated Genetic Algorithm," *Proceeding of the 1st International Conference on Genetic Algorithms*, Lawrence Erlbaum Assoc., Mahwah, NJ, 1985, pp. 93–100.

[22] Fonseca, C. M., and Fleming, P. J., "Genetic Algorithms for Multi-Objective Optimization Formulation, Discussion, and Generalization," *Proceedings of the 5th International Conference on Genetic Algorithms*, Morgan Kaufmann, San Mateo, CA, 1993, pp. 416–423.

[23] Srinivas, N., and Deb, K., "Multi-Objective Function Optimization Using Nondominated Sorting Genetic Algorithms," *Evolutionary Computation*, Vol. 2, No. 3, 1995, pp. 221–248.

[24] Narayanan, S., and Azarm, S., "On Improving Multi-Objective Genetic Algorithms for Design Optimization," *Structural Optimization*, Vol. 18, Nos. 2–3, 1999, pp. 146–165.

[25] Crossley, W., Cook, A., Fanjoy, D., and Venkayya, V., "Using the Two-Branch Tournament Genetic Algorithm for Multi-Objective Design," *AIAA Journal*, Vol. 37, No. 2, 1999, pp. 261–267.

[26] Coverston–Caroll, V., Hartmann, J. W., and Mason, W. J., "Optimal Multi-Objective Low-Thrust Spacecraft Trajectories," *Computer Methods in Applied Mechanics and Engineering*, Vol. 186, No. 2, 2000, pp. 387–402.

[27] Deb, K., Pratap, A., Agarwal, S., and Meyarivan, T., "A Fast and Elitist Multi-Objective Genetic Algorithm: NSGA-2," *IEEE Transactions on Evolutionary Computation*, Vol. 6, No. 2, 2000, pp. 182–197.

[28] Michalewicz, Z., Janikow, C., and Krawczyk, J., "A Modified Genetic Algorithm for Optimal Control Problem," *Computers & Mathematics with Applications*, Vol. 23, No. 2, 1992, pp. 83–94.